Distribution Agreement

In presenting this thesis as a partial fulfillment of the requirements for a degree from Emory University, I hereby grant to Emory University and its agents the non-exclusive license to archive, make accessible, and display my thesis in whole or in part in all forms of media, now or hereafter know, including display on the World Wide Web. I understand that I may select some access restrictions as part of the online submission of this thesis. I retain all ownership rights to the copyright of the thesis. I also retain the right to use in future works (such as articles or books) all or part of this thesis.

Siddharth Raju 3/29/2016

Determination of Order in Desmosomes and Resolution of Mechanisms of Pemphigus Vulgaris

By

Siddharth Raju

James Nagy
Adviser

Department of Mathematics and Computer Science

James Nagy
Advisor

Alexa Mattheyses
Committee Member

Eric Weeks
Committee Member

2016

Determination of Order in Desmosomes and Resolution of Mechanisms of Pemphigus Vulgaris

By

Siddharth Raju

James Nagy
Adviser

Abstract of
A thesis submitted to the Faculty of Emory College
of Emory University in partial fulfillment
of the requirements of the degree of
Bachelor of Sciences with Honors

Department of Mathematics and Computer Science

2016

Abstract

Determination of Order in Desmosomes and Resolution of Mechanisms of Pemphigus Vulgaris
By Siddharth Raju

Desmosomes are dynamic, adhesive, intercellular junctions that provide mechanical stability for skin. This stability is undermined by the autoimmune disorder Pemphigus Vulgaris (PV). Previous work has found evidence to suggest that PV interferes with desmosomal adhesion and in this manner undermines mechanical stability of skin. We hypothesize that healthy skin contains "ordered" desmosomes while diseased skin contains "disordered" desmosomes, and that the main mechanism of PV is to destroy the structure of ordinarily ordered junctions which provide the strongest possible adhesion. To this end we have developed mathematical models to understand the dynamics of the desmosome system and analyzed the subsequent simulated data to investigate how order may arise.

Determination of Order in Desmosomes and Resolution of Mechanisms of Pemphigus Vulgaris

By

Siddharth Raju

James Nagy
Adviser

A thesis submitted to the Faculty of Emory College
of Emory University in partial fulfillment
of the requirements of the degree of
Bachelors of Science with Honors

Department of Mathematics and Computer Science

2016

Contents

List of Figures

Chapter 1

Introduction

1.1 Biological Background

Skin is our body's basic defense against external disturbances, providing mechanical and infectious resistance. We are able to tolerate small perturbations without major loss in biological operation due to this defense [5]. However, this defense can break down in the face of autoimmune diseases both inherited and acquired. One autoimmune disease, Pemphigus Vulgaris (PV) leads to blistering and erosion in the skin [4]. In order to develop targeted treatments that address the source of the problem, for present treatments can only address symptoms, we require a better understanding of how PV disrupts the skin's defenses. We seek to uncover the underlying mechanisms of PV responsible for this breakdown.

As a starting point, we need to consider desmosomes, adhesive junctions present in skin cells which are the basic components that confer mechanical strength to skin [13]. These intercellular junctions distinguish themselves from others in that they can achieve a significant adhesive state which acts as a bulwark against mechanical strain [7]. The proteins most associated with this type of junction are known as desmogleins. Furthermore, desmosomes are dynamic; they can switch between low and high adhesive states [7]. A detailed illustration is provided in Figure 1.1.

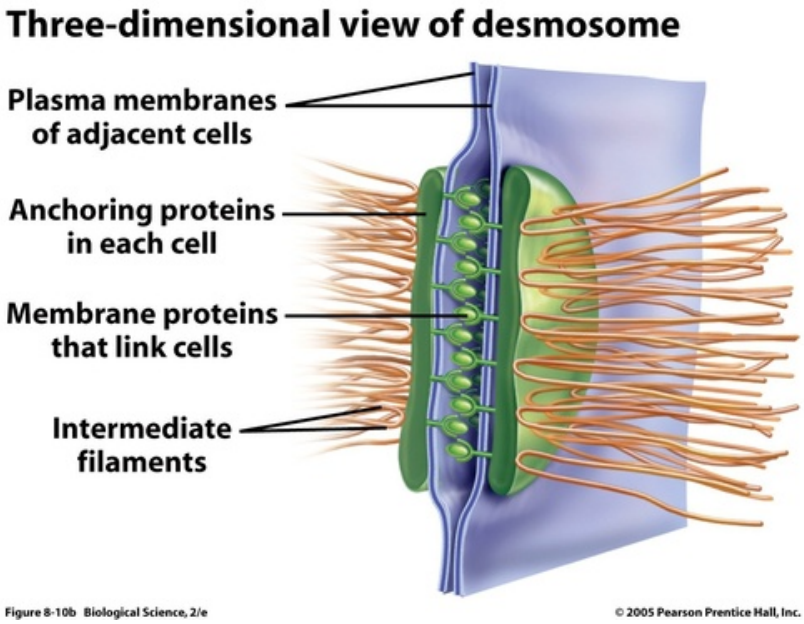

Figure 1.1: The desmosome is a highly specialized adhesive junction that links cellular domains. Its ability to provide skin mechanical resistance arises from its structure of externally connected membrane proteins between plasma membranes, anchored by proteins within each cell.

The molecular architecture of desmosomes was studied by Nekrasova and Green [19], who found that the resistance of desmosomes arises out of specialized proteins present within the cell. We will delve into this architecture in section 1.2 when we present our preliminary steps.

Previously, the work that has been done to understand the desmosome has used bulk assays and standard microscopy techniques. For instance, Maynadier et al showed that increased cell-cell adhesion in these cells is caused by increased desmosome formation using dissociation assays [18]. Al-Amoudi and Frangakis, through electron microscopy, were able to describe the architecture of the junction [2]. Further work by Al-Amoudi et al used electron microscopy to observe the extracellular space of the junction and suggested that there may be an intrinsic ordering in the system[1]. Such studies have laid the groundwork for our understanding of the desmosome and

its role in adhesion and mechanical stability. Our goal is to study the organization and dynamics of desmosomal proteins in living cells.

Much research has also been done regarding the influence of PV on desmosomes. Jones et al have shown that PV specifically recognizes desmosomes and directs antibodies to bind to the desmosomes [9]. This tells us that PV directly interacts with desmosomes, and Amagai et al have shown more specifically that it is the specific protein desmoglein 3 (Dsg3) which is the target [3]. Desmogleins are the proteins most important for adhesion according to experiments by Koch et. al [12]. Through standard imaging of diseased cells in mice, Shimizu et al showed that the extracellular domain bindings of Dsg3 are actually split by pemphigus [20]. In sum, PV attaches to the most important proteins required for adhesion, and the protein bindings show damage after a sufficiently long time.

We have good reason to believe, based on these studies, that PV works in part through direct disruption of proteins on the desmosome and in doing so causes the blistering and erosion it has been formerly associated with. We move forward in our work with the confidence that it is indeed the disruption of desmosomal adhesion that leads to the symptoms of PV and formulate our models with this assumption as our guide.

The reader at this point might certainly ask why no work has yet been done on observing PV in action; we have a good deal of data to support the claim that PV in some way binds to and directly disrupts the desmosome, but we have not actually seen in what way this disruption is achieved between the initial step where we see the bound desmosome and the final step where we see the disrupted desmosome. The answer is, primarily, practicality. Dissociation assays can give a bulk measurement of adhesion for a cell population, but cannot measure the adhesion of individual cells. Electron microscopy allows fixed and detailed observation of samples, but does not

allow for dynamic viewing. This limitation has left a gap in the knowledge of this system and its disruption by PV, and it is the goal of the technique that we have invented (to be presented shortly) to address this knowledge gap. The entirety of this research effort, in fact, is in pursuit of this goal. We will see later that this technique can find a home in many other fields.

1.2 Hypothesis and Method Background

A central dogma of biology is that structure and function are intertwined. When we consider the structure of the desmosome, we notice that it relies heavily on its membrane proteins for adhesion (Figure 1.1). We propose that this adhesive strength depends on a highly ordered ensemble of protein clusters. Based on the picture of Figure 1.1 we present an organizational model based on our understanding of previous work (Figure 1.2). Desmogleins and desmocollins (which are the membrane proteins) attach to each other in the extracellular space, and are anchored in each cell by another set of proteins known as plakoglobins (hexagons), plakophilin (big circles), and desmoplakin (crossed lines). Our idea of order depends on a rigidity in membrane proteins provided by the intracellular proteins that is invariant in orientation across each membrane protein.

If this supposed ordering of the membrane proteins were somehow disrupted (a change in structure), we would expect a change in the function of the desmosome, most likely that adhesion and mechanical resistance would be weaker as is characteristic of skin cells infected by PV. In light of the evidence presented in section 1.1, this hypothesis has a firm foundation. With these ideas in mind, we formulate our hypothesis.

For our purposes, we simplify the pictures of Figure 1.1 and Figure 1.2 to con-

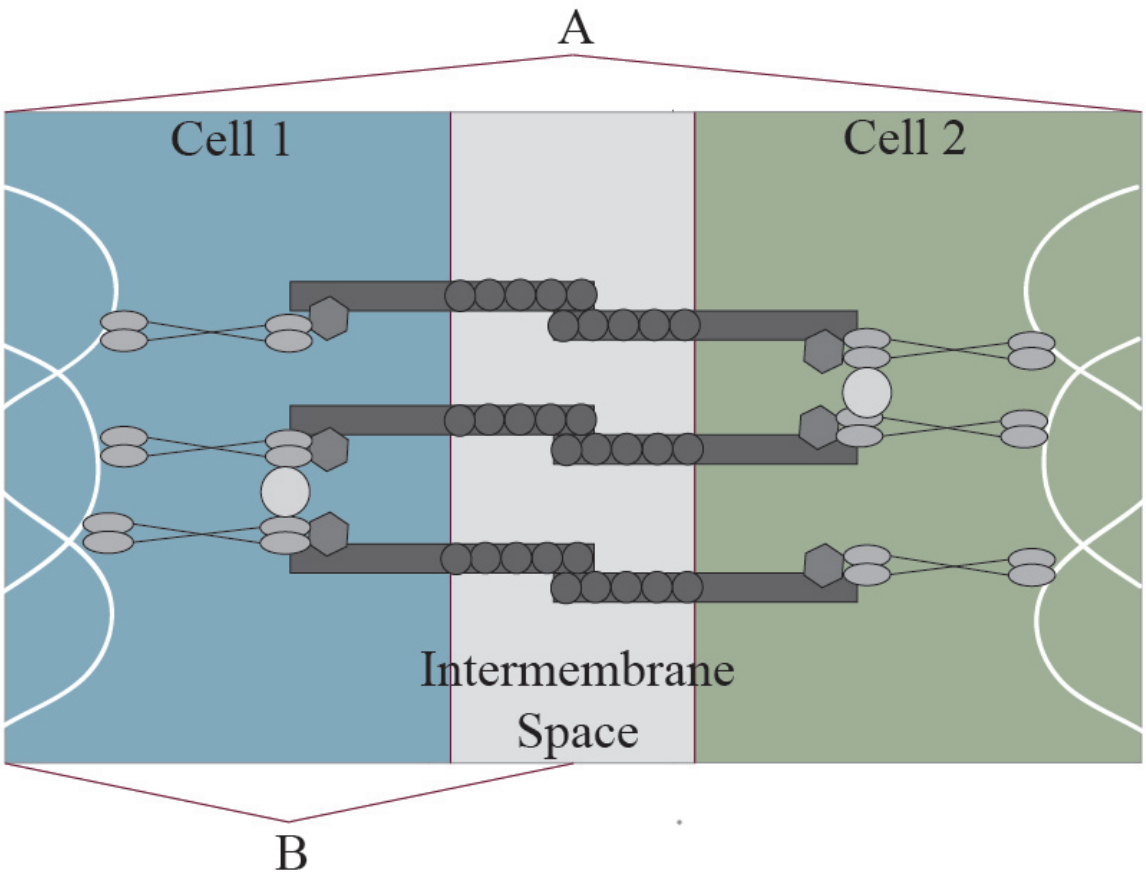

Figure 1.2: Desmogleins and desmocollins (membrane proteins) bind to each other in the extracellular space, anchored by a variety of proteins inside each constituent cell: plakoglobins (hexagons), plakophilin (big circles), and desmoplakin (crossed lines). This picture describes our idea of how order manifests in desmosomes.

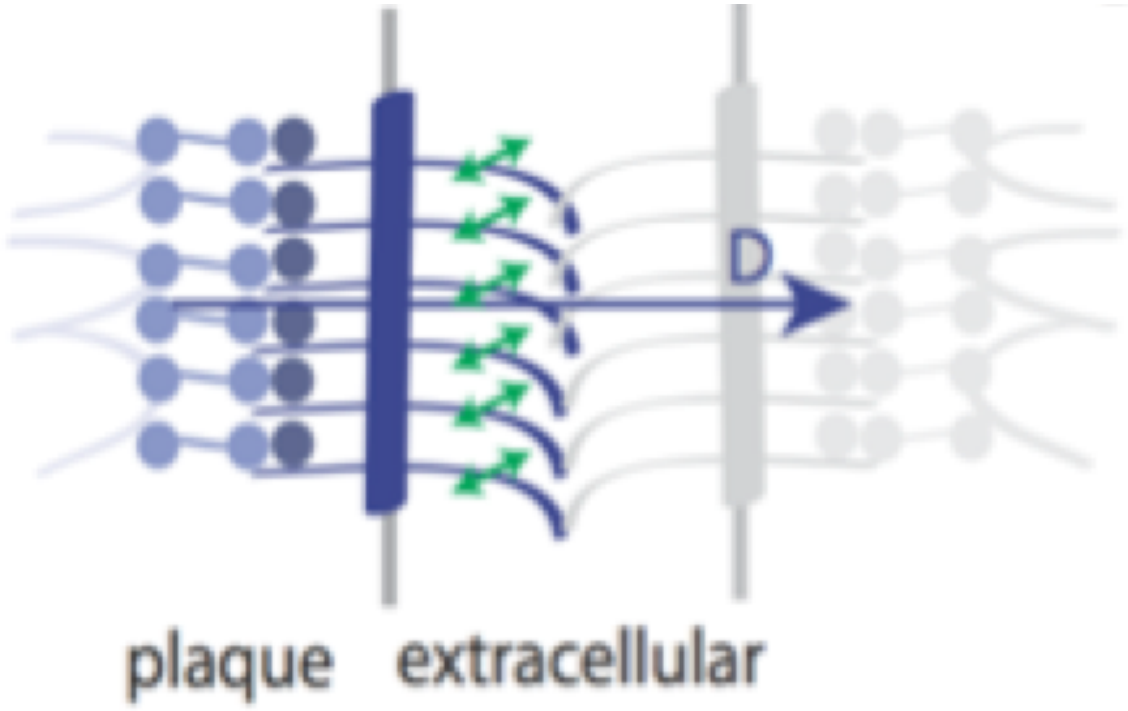

Figure 1.3: Simplified view of the desmosome, for modeling purposes The proteins along the desmosomes are like a"mesh" that confers stability and allows for adhesion between the plaque and extracellular domains.

ceptualize desmosomes as sets of proteins jutting out from the plasma membrane, providing adhesive support by connecting plaque and extracellular domains (Figure 1.3). For now, we will assume that they are rigidly held in place by the intracellular proteins and adhesion.

We hypothesize that the adhesive strength of the binding is directly related to the relative order of those proteins. We define the order of the system to be the degree to which all the proteins in a desmosome are oriented in the same direction. Thus, the strongest system has all of its proteins oriented in the same direction, while the weakest system has its proteins oriented completely randomly. If this hypothesis is true, then it should be the case that desmosomes of healthy skin cells are ordered, while the desmosomes of skin cells infected by PV are disordered; we seek to show

that fundamentally what PV does is destroy the structure of what was a healthy, ordered desmosome by interfering with its membrane proteins. By measuring the ordering of these two systems, we will be able to test our hypothesis.

To measure the ordering of these two different systems, we use the method of fluorescence polarization. The basic idea behind fluorescence polarization is that the proportion of incident light returned by a fluorescently tagged protein, like green fluorescent protein (GFP), will be dependent on the relative orientation of the polarized light and the given protein; specifically, the probability of excitation is proportional to $\cos^2(\theta)$, where θ is the angle between the excitation dipole of the protein (a specified spatial orientation that maximizes excitation) and the polarized light. Physicists will recognize this statement as Malus' Law. Inherent in this approach is the assumption that proteins are rigid, for the technique relies on the excitation dipole remaining constant relative to the protein being studied.

The experimenter has the ability to change the polarization of excitation light; by measuring the proportion of incident light returned (fluorescence intensity) at different polarization angles, the experimenter can empirically find the peaks of returned incident light (this is when the orientation of light and the excitation dipole are most similar) to determine the structure at the molecular level. In biochemical contexts, fluorescence polarization has been used to study activity at the molecular level [16]. By combining this technique with microscopy, we can reveal spatial information at this scale.

Kampmann et al have successfully used the technique to map the orientation of nuclear pore proteins in living cells [11], while Mattheyses et al have revealed order and disorder of protein domains in the nuclear pore complex [17]. The fundamental similarity between these applications is that the system being studied exhibits some natural order. Furthermore, Kress et al have used excitation-polarization-resolved

confocal fluorescence microscopy to map the local organization of cell membranes [15] and have also probed molecular orientational order of rigid proteins [14]. DeMay et al have even observed ordered septin dynamics in live yeast by the same method [6]. Suffice it to say, the method has been shown to be powerful in a variety of contexts (particularly for mapping domains and determining order), and can easily be repurposed to the task at hand of determining the order of dynamic protein clusters between the plasma membranes of skin cells.

We can adopt this technique for our purposes if we recall that the desmosome contains sets of proteins along the cell's plasma membrane that bridge domains; if the system is in fact ordered, then fluorescence polarization ought to reveal the order to us. If the proteins are all disordered, the fluorescence intensity should be independent of the polarization angle of the excitation light (there is no "peak"). We thus apply the technique to both healthy and diseased cells, expecting the polarization to show order for healthy cells and show disorder for diseased cells. Because fluorescence polarization can even allow for dynamic observation, we will be able to address the aforementioned limitation in observation and for the first time be able to investigate the mechanisms of PV between binding and final disruption. We aim to ultimately describe in fine detail the mechanisms of PV, a previously unattainable feat.

This technique as applied to this system and our corresponding analysis is novel, and we hope that the reader will understand the power of the technique and analysis in the coming pages.

Chapter 2

Modeling

2.1 Spatial Analysis

In this section, we define a coordinate system for desmosome. This coordinate system will allow us to discuss more precisely the concept of order and lead us to the tools we need in order to ultimately understand the mechanisms of PV.

Consider the desmosome system superimposed with the coordinate system given in Figure 2.1. Given a cell in the light microscope coordinate system x-y-z, x-y is the plane of observation and z is perpendicular to this plane. For any given desmosome, D, the desmosome axis, is perpendicular to the plasma membrane of the cell and lives in the x-y plane. The angle between D and the x-axis is given by γ. The vector representing the polarization of the excitation light, ϵ, lives in the x-y plane and the angle between ϵ and D is given by ω. F is chosen to coincide with the z-axis, and E is coplanar and perpendicular to D, so that we may define an alternative 3D space of Cartesian coordinate: D-E-F. The reason for this shift is so that we can consider multiple sets of proteins along a single observation plate by simply redefining D while keeping x and y constant.

The transition dipole of a fluorophore fixed within the desmosome is μ. The orientation of μ within the desmosome is described by two angles: the polar angle α

between μ and D and the azimuthal angle βbetween F and the projection of μ onto the EF plane. We expect a degree of symmetry about the desmosome axis, which is why we have switched the classic definitions of the azimuthal and polar angle to make D the "special" axis instead of F; the following results with the standard definition are considered in section 2.5.

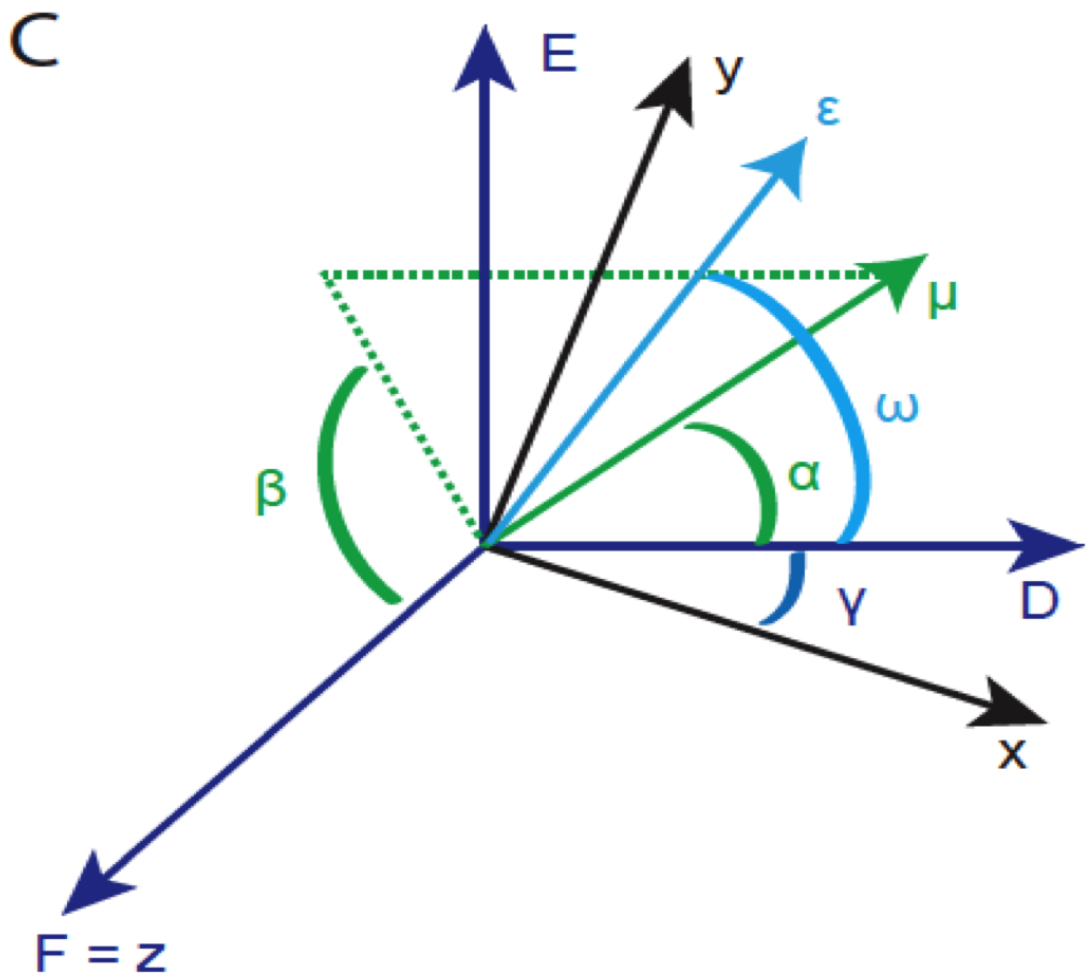

Figure 2.1: A mathematical representation of the desmosome system. The x-y plane denotes the plane of observation, while the z axis is parallel to the line of sight from the microscope. The D axis lies normal to the plasma membrane and points in the direction of the desmosome's orientation. Together with E, it forms a plane rotated by an angle γ from the plane of observation, while F lies along z. ϵ denotes the polarization of light in the observation plane and is defined by an angle ω. Finally, μ is the tagged protein, defined spatially by the polar angle α and the azimuthal angle β.

2.2 Intensity Function

The above definitions coupled with our understanding of light polarization and electromagnetic energy yield an intensity function that models the proportion of incident light we ought to receive back as a signal from a single protein given a spatial orientation (α, β) and polarization angle (ω):

$$\begin{aligned} P(\alpha,\beta,\omega) &= \cos^2(\alpha)\cos^2(\omega) + 2\cos(\alpha)\cos(\omega)\sin(\alpha)\sin(\beta)\sin(\omega) \\ &\quad + \sin^2(\alpha)\sin^2(\beta)\sin^2(\omega) \end{aligned}$$

For the case of light returned from a set of proteins (the entire desmosome), we would find that for a set of protein orientations described by $\vec{\alpha}$ and $\vec{\beta}$

$$\begin{aligned} P(\vec{\alpha},\vec{\beta},\omega) &= \frac{1}{p}\left(\cos^2(\omega)\sum_{i=1}^{p}\cos^2(\alpha_i) + 2\sin(\omega)\cos(\omega)\sum_{i=1}^{p}\sin(\alpha_i)\sin(\beta_i)\cos(\alpha_i)\right. \\ &\quad \left. + \sin^2(\omega)\sum_{i=1}^{p}\sin^2(\alpha_i)\sin^2(\beta_i)\right) \end{aligned}$$

where p is the number of proteins on the desmosome, α_i is the α angle of the i^{th} protein, and β_i is the β angle of the i^{th} protein. The details of these derivations can be found in the next section. Since α and β are constants defined by the system, we see that the proportion of light returned is dependent only upon the angle of polarized light, as was predicted in the introduction.

Sample plots for ordered populations, that is, sets of proteins with uniform orientations, are shown in Figure 2.2. Note how each plot has a curve that varies from its average line over the range of polarization angles. By contrast, desmosomes populated by disordered proteins do not exhibit this same curving behavior (Figure 2.3).

Using this result, we are able to understand a few things about the system, which

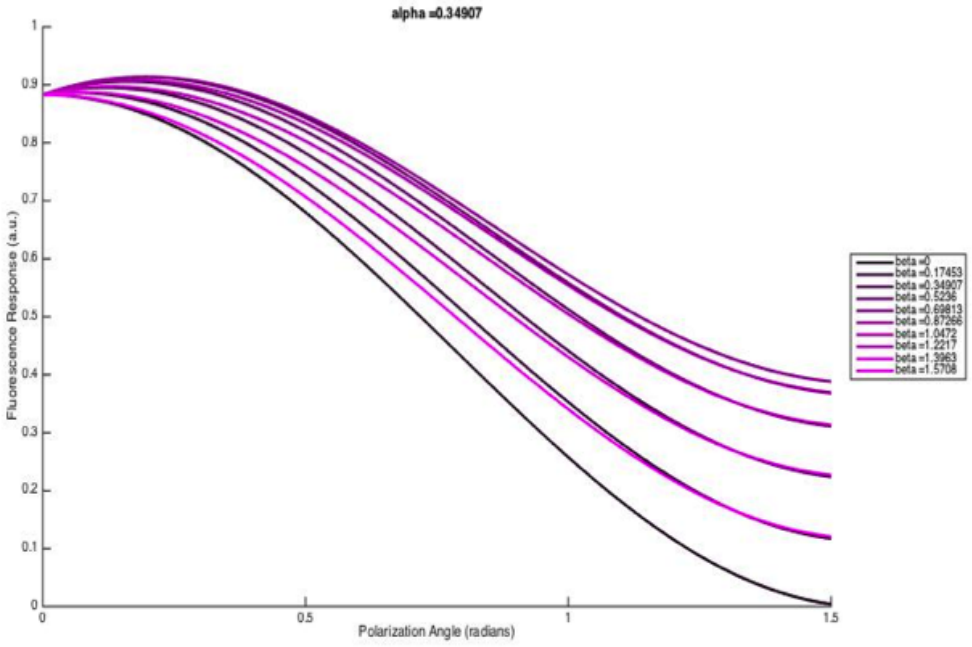

Figure 2.2: Sample plots of intensity function for a fixed α and varying β over a range of polarization angles ω. There is a clear variation over the set of polarization angles for each of these plots, but some orientations yield more variable curves.

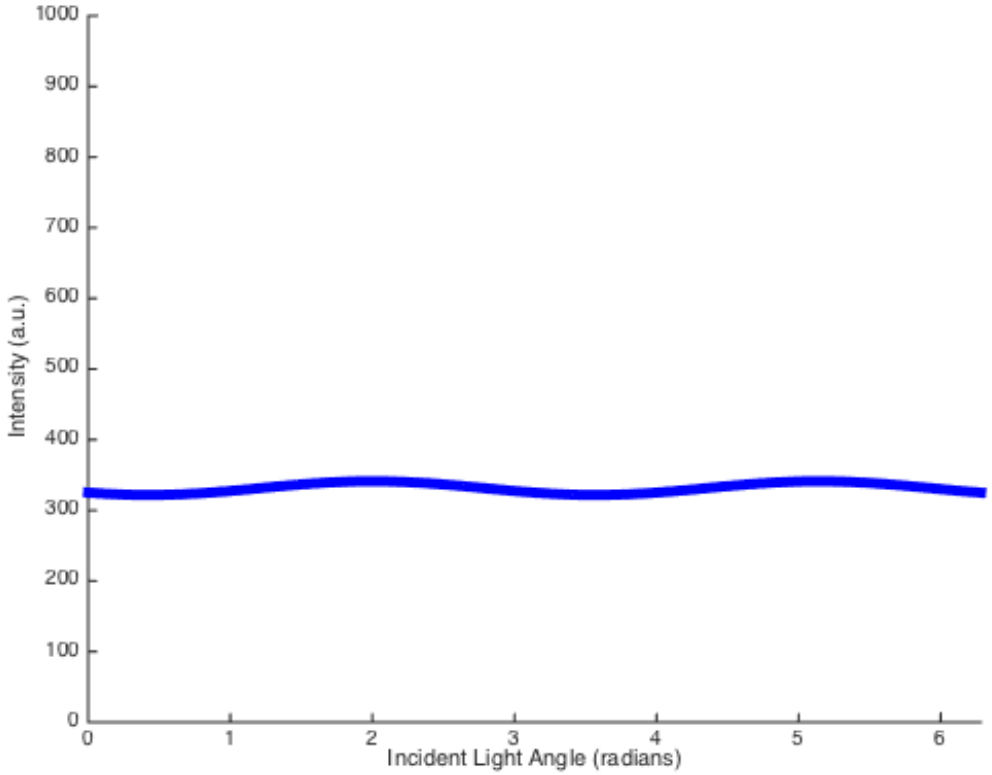

Figure 2.3: Disordered populations do not exhibit large variations from a flat line.

are expounded upon in greater detail in section 2.4.

2.3 Derivations

2.3.1 Derivation of Intensity Function for a Single Protein

Reference Figure 2 for definitions of ω, α, ϵ, μ, and β. Here, we assume that $\gamma = 0$ for simplicity, but the result easily generalizes for arbitrary γ, up to a phase shift.

We can write

$$\vec{\epsilon} \equiv (\cos(\omega), \sin(\omega), 0)$$

as the **polarization vector**, which can describe any light polarization direction in the xy-plane.

Further, we can express

$$\vec{\mu} \equiv (\cos(\alpha), \sin(\alpha)\sin(\beta), \sin(\alpha)\cos(\beta))$$

which describes any orientation of a fluorophore rigidly attached to the *desmosome*.

If light is polarized in $\vec{\epsilon}$, then for each *individual* fluorophore, the probability P_μ of being excited by the polarized light is proportional to ${\mu_\epsilon}^2$ (the projection of $\vec{\mu}$ along $\vec{\epsilon}$) since the energy of an electric field is proportional to the square of the electric field and the probability of excitation is proportional to the energy of the electric field:

$$P_\mu \propto {\mu_\epsilon}^2$$

By the definition of projections, we have

$$\mu_\epsilon = \frac{\vec{\mu} \cdot \vec{\epsilon}}{\|\vec{\mu}\|\|\vec{\epsilon}\|}$$

$$\|\vec{\mu}\| = \sqrt{\vec{\mu}\cdot\vec{\mu}} = \sqrt{\cos^2(\alpha) + \sin^2(\alpha)\sin^2(\beta) + \sin^2(\alpha)\cos^2(\beta)} = \sqrt{1} = 1$$

$$\|\vec{\epsilon}\| = \sqrt{\vec{\epsilon}\cdot\vec{\epsilon}} = \sqrt{\cos^2(\omega) + \sin^2(\omega)} = \sqrt{1} = 1$$

$$\Rightarrow \mu_\epsilon = \vec{\mu}\cdot\vec{\epsilon} = \cos(\alpha)\cos(\omega) + \sin(\alpha)\sin(\beta)\sin(\omega) \tag{2.1}$$

$$\Rightarrow \mu_\epsilon^2 = (\cos(\alpha)\cos(\omega) + \sin(\alpha)\sin(\beta)\sin(\omega))^2 \tag{2.2}$$

Because $P_\mu \propto {\mu_\epsilon}^2$, we can define a **probability (intensity) function**

$$P(\alpha, \beta, \omega) \equiv {\mu_\epsilon}^2$$

that will represent relative probabilities of excitation (and, ultimately, proportional intensity of excitation response from a group of fluorophores within some neighborhood).

Therefore,

$$\begin{aligned} P(\alpha,\beta,\omega) &= \cos^2(\alpha)\cos^2(\omega) + 2\sin(\alpha)\sin(\beta)\sin(\omega)\cos(\alpha)\cos(\omega) \\ &\quad + \sin^2(\alpha)\sin^2(\beta)\sin^2(\omega) \end{aligned}$$

2.3.2 Derivation of Intensity Function for Multiple Proteins

Consider the intensity function

$$\begin{aligned} P(\alpha,\beta,\omega) &= \cos^2(\alpha)\cos^2(\omega) + 2\sin(\alpha)\sin(\beta)\sin(\omega)\cos(\alpha)\cos(\omega) \\ &\quad + \sin^2(\alpha)\sin^2(\beta)\sin^2(\omega) \end{aligned}$$

Now, we will have a set of α and β orientations ($\vec{\alpha}$ and $\vec{\beta}$) for the set of proteins present on a given desmosome. We will want to sum the intensity contribution from

each individual protein so that we can resolve the total intensity contribution from the entire desmosome. This can be written as

$$\begin{aligned} P(\vec{\alpha},\vec{\beta},\omega) &= \frac{1}{p}\sum_{i=1}^{p}\cos^2(\alpha_i)\cos^2(\omega) + 2\sin(\alpha_i)\sin(\beta_i)\sin(\omega)\cos(\alpha_i)\cos(\omega) \\ &\quad + \sin^2(\alpha_i)\sin^2(\beta_i)\sin^2(\omega) \end{aligned}$$

where p is the number of proteins. Therefore,

$$\begin{aligned} P(\vec{\alpha},\vec{\beta},\omega) &= \frac{1}{p}\left(\cos^2(\omega)\sum_{i=1}^{p}\cos^2(\alpha_i) + 2\sin(\omega)\cos(\omega)\sum_{i=1}^{p}\sin(\alpha_i)\sin(\beta_i)\cos(\alpha_i)\right. \\ &\quad \left. + \sin^2(\omega)\sum_{i=1}^{p}\sin^2(\alpha_i)\sin^2(\beta_i)\right) \end{aligned}$$

Notice that this equation reduces to the equation for a single protein in the case where α_i and β_i are constant for all i and j, which makes sense since that would denote our ordered system.

2.4 Preliminary Observations and Method Development

An observation that we make through the course of our modeling is that "not all orientations are created equal". More specifically, there exist certain orientations (α, β combinations) that exhibit behavior indistinguishable from that of a disordered system, that is to say, their curves are more "flat". The relative degree to which orientations are distinguishable is shown in Figure 2.4. The details of how this figure was created will be discussed later.

The number of photons we observe coming from the fluorophore given our incident

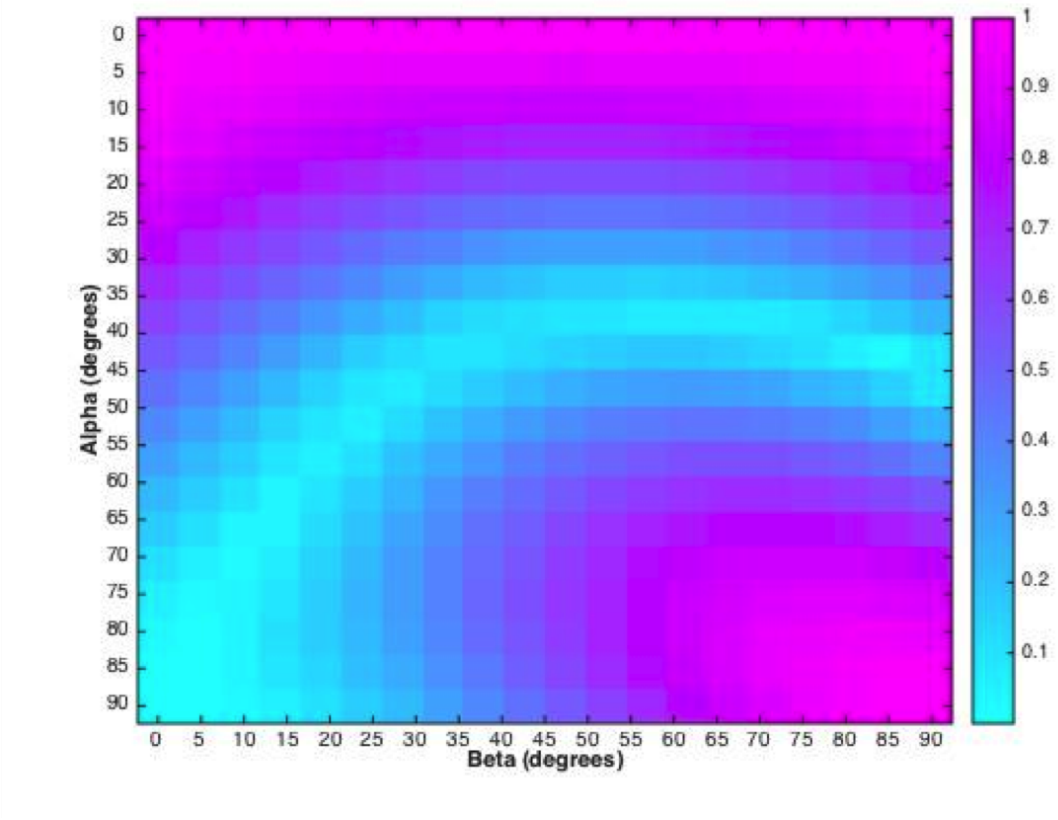

Figure 2.4: Illustrates the different "visibility" of different orientations against a disordered case. Even though a desmosome system is ordered, it may not appear so under the method of fluorescence polarization. Certain orientations are much harder to detect than others, so it can be the case that fluorescence polarization gives us a null result even though the system truly is ordered, which we would call a Type II error.

intensity level depends primarily on relative positioning of the light's polarization and the plane orientation of the fluorophore. However, we know that there is a certain variability that can occur in the reading of an observation device due to the particle nature of light [10], so we account for this variance in our model by taking the observed result to be randomly drawn from a Poisson distribution with its parameter set to the ideal value as is standard [10].

We want to find a method by which we can differentiate ordered populations from disordered populations by using only a few intensity values from a given population. The algorithm for determining the appropriate cutoff is presented in the coming paragraphs. Before moving on to the method, however, we must first take a detour to introduce the concept of a spline.

Consider the problem of interpolation, that is, attempting to predict system behavior between data points. In many experiments (perhaps even most) taking the data of a system at every point of interest is not feasible, so we must rely on interpolation techniques to predict behavior between discretely spaced data points. One such technique is that of cubic spline interpolation, which has been shown to be robust and reliable. In essence, the behavior between data points is modeled by a collection of third degree polynomials[7]. Figure 2.5 shows an example of the spline in action.

A more detailed treatment can be found in Introduction to Scientific Computing Using MATLAB [8]. For now, we move onto the method.

We first create a large sample ($n = 400$) of orientations from the entire possible set of orientations. For each of these orientations, we create a population of 500 proteins that all point in the same direction and record the noise-injected intensity by plugging in the spatial coordinates to the intensity function at five polarization angles ($w = 0$, $\pi/8$, $\pi/4$, $3\pi/8$, $\pi/2$) and generating a random number from the Poisson distribution with the intensity function's output as the parameter.

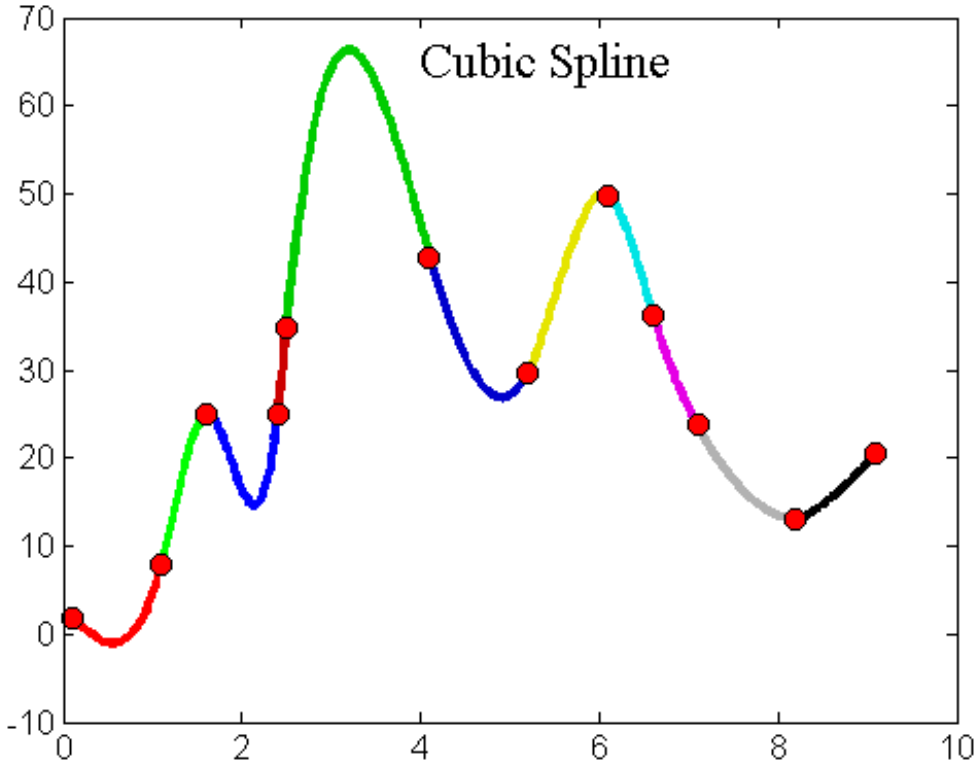

Figure 2.5: An example of how a cubic spline interpolates given data points. The curve is made up of piecewise continuous third order polynomials defined by the data points. Credit: profmsaeed.org

The reason why we choose only five data points is that we want to simulate the actual experiment as much as possible, and an actual experiment would not allow us to take arbitrarily many data points. This is because excessive stimulation of a fluorophore will eventually make it lose its ability to fluoresce; this is a phenomenon known as photobleaching [21]. Thus, we need a way to predict the system's order based off of only a few data points, and the spline is the tool that lets us do so.

Once we have created a spline to interpolate the data, we find the average value of the spline curve and record the area between the spline curve and the average line (Figure 2.6). Large areas signify order, while small areas signify disorder. The intuition behind this method is that a disordered population would yield a nearly flat curve subject to Poisson noise; a good deal of variation from a flat line gives evidence of ordering, and a greater degree of variation should indicate a greater degree of ordering. This fact becomes even more apparent at higher intensity values, where the noise due to Poisson becomes less important (Figure 2.7) since the main signal intensity scales with the incident intensity, while the noise scales only with square root of incident intensity.

For an illustration, return to Figure 2.4. For a given population with a uniform orientation defined by α and β, we perform the above procedure to associate an area with each orientation in the α, β matrix. The resultant "heat map" represents how obviously a given population is ordered relative to another.

We repeat this procedure for populations of disordered proteins, that is to say, a set of proteins who all have different orientations. Using this data, we then go about finding an appropriate cutoff area value by considering Type I and Type II errors. More specifically, for a chosen cutoff value c, if the area between the spline curve and its average line is greater than c, then we declare the system responsible for that curve to be ordered. If it is lower than or equal to c, then that system is declared

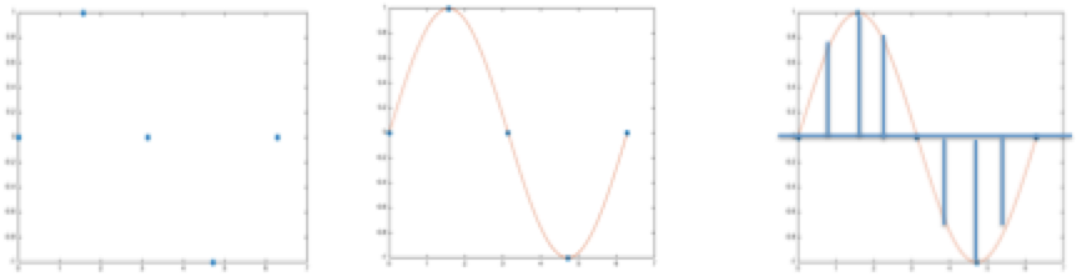

Figure 2.6: We start with our five data points for a given trial. We use a cubic spline to interpolate those five data points, and then record the area between the curve and the average line for that curve. This area is the crucial measurement for our final determinations of order.

disordered. A Type I error would be declaring a disordered protein ordered when it is actually disordered, while a Type II error would be declaring an ordered protein disordered when it is actually ordered.

We compute the error percentages for a given cutoff by comparing the cutoff to the recorded area for each population (ordered or random), and recording whether or not that population would pass the test at that particular cutoff. An illustration of modeled results can be found in Figure 2.8.

We have performed this procedure for light of varying amplitudes, and have found that the ideal cutoff which minimizes both Type I and Type II errors-when divided by the associated amplitude-is about 3.4.

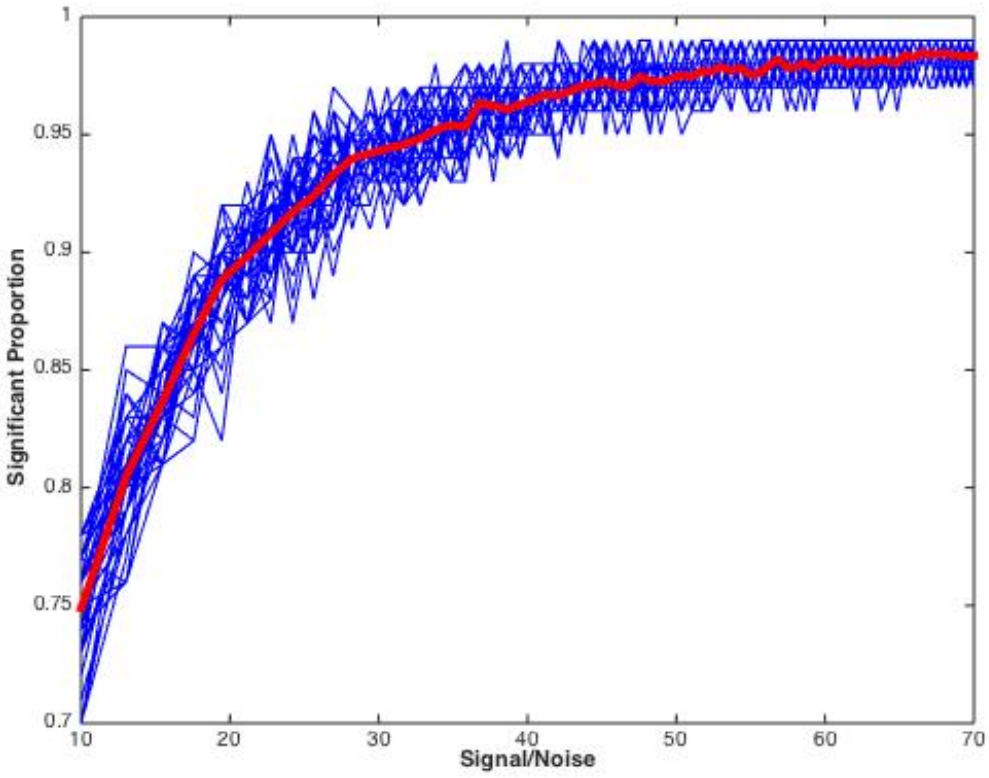

Figure 2.7: This graph shows what proportion of ordered populations are declared ordered under our method as our intensity increases (and noise becomes less important). Clearly, the method is more powerful at higher intensity levels, when the signal dominates the noise.

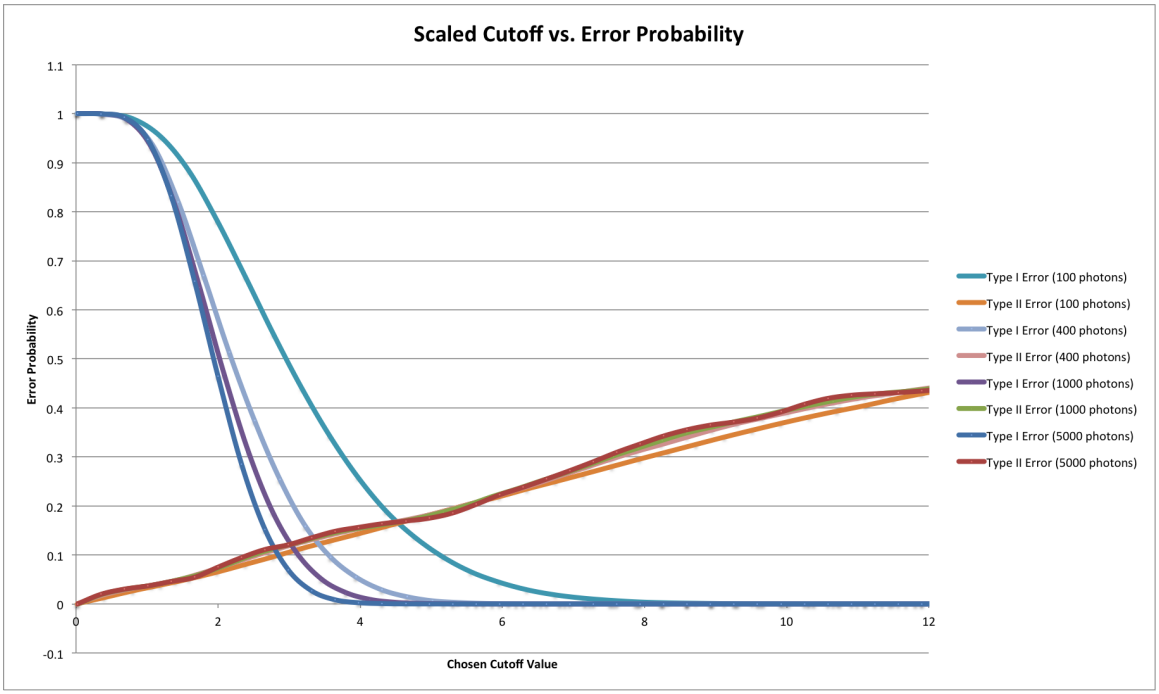

Figure 2.8: At low cutoff values, Type I errors are very common, while Type II errors are rare. As the cutoff increases, Type I errors go to 0, but Type II errors become prevalent. The cutoff must be chosen large enough so as to not overstate significance, but also small enough so as to not out of hand reject significant data.

2.5 Alternative Formulation

Following the same steps as in section 2.3 with β chosen to be the polar angle and α the azimuthal angle, we obtain an intensity function of

$$P(\alpha, \beta, \omega) \quad = \quad \sin^2(\beta)\cos^2(\alpha - \omega).$$

This formulation is much cleaner, and makes more apparent the use of Malus' Law in our technique. The reason we have not used this method in our technique is because of the symmetry involved in the biological system referenced earlier in section 2.1. However, this formulation is useful in that it lets us consider another method to test significance: least-squares fitting. In Figure 2.9, ten noisy data points are generated from the new intensity function for $\alpha = \pi/3$ and $\beta = \pi/4$ and plotted over the range $\omega = 0$ to $\omega = \pi$. We have fitted the data points to a function of the form

$$I = A\cos^2(\alpha - \omega)$$

which is in fact just a version of Malus' Law and clearly fits the data well. Our alternative test could be how well the data fits a cosine squared curve; if the fit is good, the data is likely ordered. If the fit is bad, then the data is more likely disordered (i.e. not giving characteristic peaks). An example of a cosine fit to disordered data can be found in Figure 2.10, where the fit is laughable.

In some sense, the area test and least-squares fitting are related; the area test associates large areas with order while the least-squares fitting associates closeness to a cosine squared curve with order. Because data that more closely resembles a cosine squared curve will necessarily have a larger area under the area test, we find that we

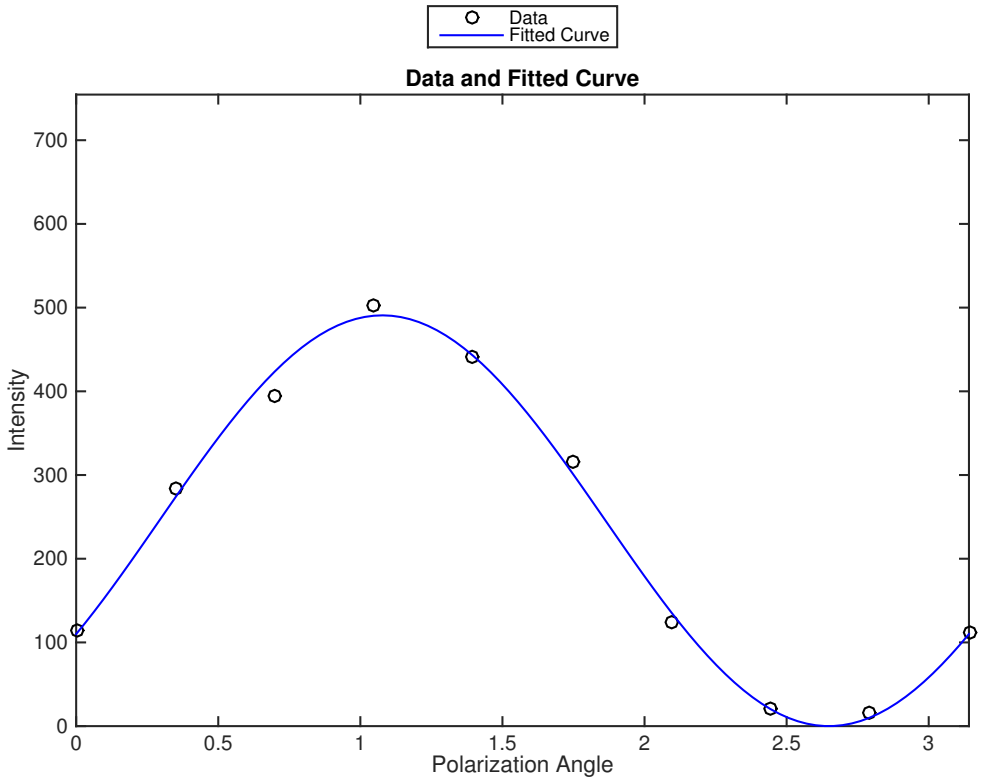

Figure 2.9: A least-squares fit of noisy data to a function of the form $A\cos^2(\alpha - \omega)$ is applied for data from a system with $\alpha = \pi/3$ and $\beta = \pi/4$. The fit is very good, as we should expect given the nature of our system and technique.

can map the significance of one method to the other. The consistency in interpretation between both formulations of the intensity function and their corresponding analyses lends credence to our technique and should give the reader more intuition about the technique's validity.

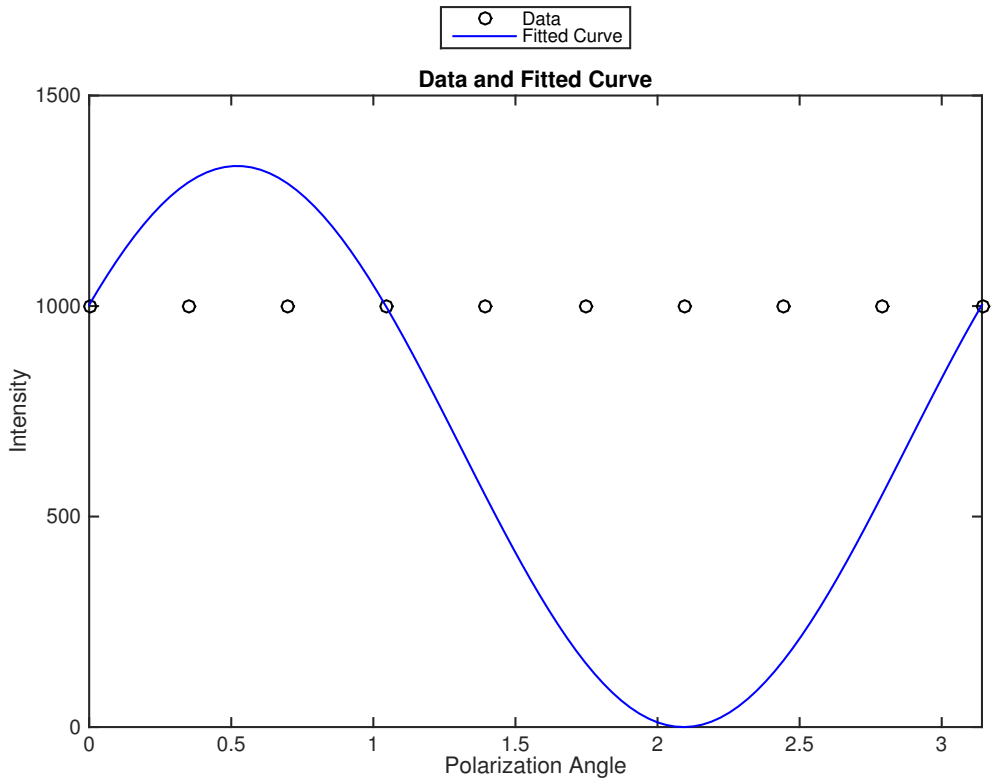

Figure 2.10: A least-squares fit of noisy data to a function of the form $A\cos^2(\alpha - \omega)$ is applied to disordered data. The fit is incredibly bad, as we should expect for disordered data.

Chapter 3

Experiment

3.1 Apparatus

We now delve into how the previously stated theoretical results play into our experiment. Our experimental apparatus is shown in Figure 3.1. We polarize the light incident upon the plane of the cell at different angles and measure the fluorescence intensity at each of these angles using a microscope-assisted camera. Polarization is achieved using the polarizer and half-wave plate. The AOTF acts as a shutter, while a CCD camera records the excitation responses.

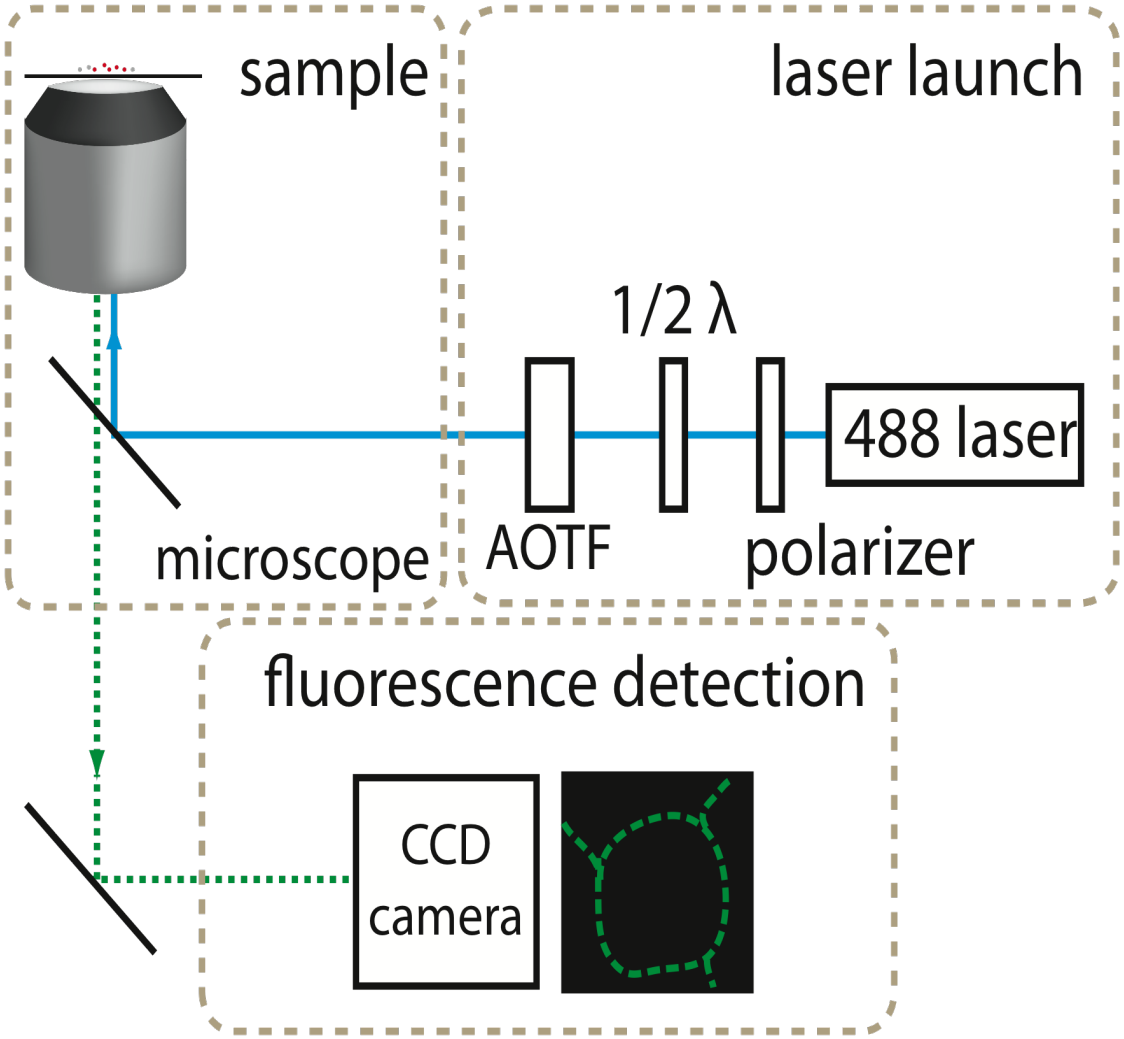

Figure 3.1: Laser light is polarized with the joint action of the polarizer and half-wave plate, while the AOTF acts as a shutter. The now polarized light is sent to the sample to excite the tagged proteins. The light is absorbed and re-emitted by the fluorophores, and a CCD camera records the relative intensity of response. This recording is performed for each angle of interest on the given system.

We translate the raw image data into a form that we can analyze and compare to our modeled results.

3.2 Data Extraction

We know empirically that our procedure applied to a null case sample of a dilute solution of fluorophores will yield data that exhibits a periodic nature due to the transmission properties of our microscope; polarization depends in part on transmission properties, and we would see oscillations as the angle is changed in the null case. To correct for this alteration-for the polarization response should be constant for the null case-we divide the matrices representing our pictures by the corresponding null case matrices. Applying these corrections to the null cases, of course, yields corrected images that are independent of polarization angle, as we wanted. In this way, we remove bias from the system.

The method by which we extract intensity values from regions of interest is as follows (Figure 3.2). First, the user draws a box around the particular region of interest on the corrected image. Next, the program zooms in on the selected region and allows the user to define a more precise subset of that region. Finally the program prompts the user to define the D vector. From here, the program takes an average of all the pixel intensity values in the selected region (excluding the outliers) and returns this average as the intensity value for that region. This same procedure is done automatically on the same region in corrected images taken at different polarization angles. In this way, one intensity value is extracted for each polarization angle, allowing the analysis to proceed as was modeled earlier.

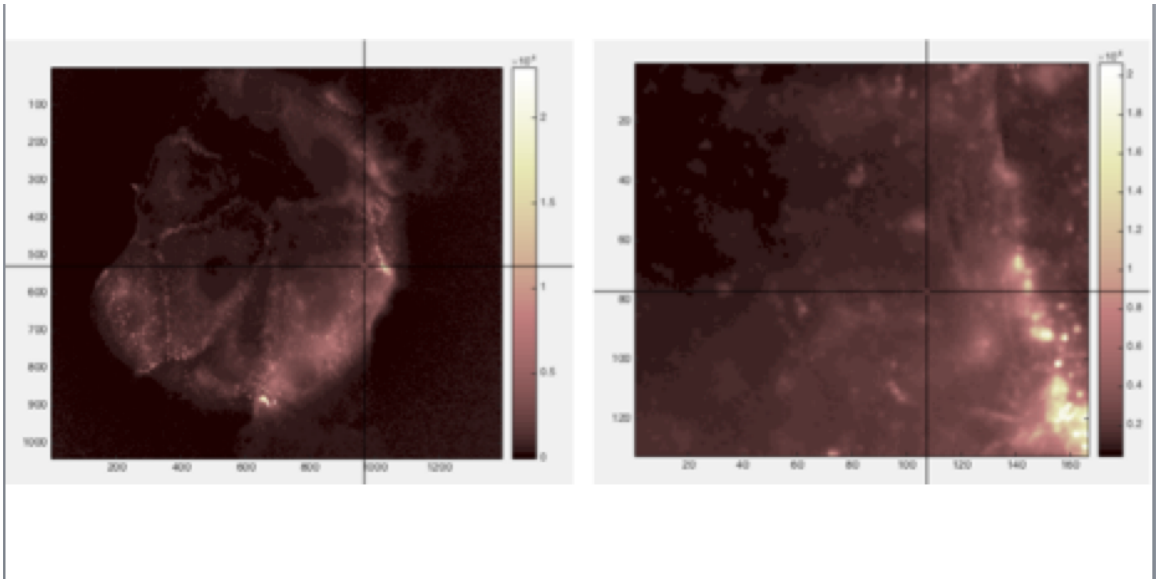

Figure 3.2: We start with the corrected image of the cell for a single polarization angle. Then we zoom in on the region of interest, and are then able to more precisely choose the area that we want to analyze. The representative pixel intensity values of this final region are averaged, and a single value is extracted and associated with the given polarization angle.

3.3 Final Analysis

The analysis method is similar to the method of cutoff determination described earlier. We create an interpolating cubic polynomial spline through the five (corrected) data points, and measure the area between the spline curve and the average line of the five responses. We compare this area to our chosen cutoff value, and from here make the determination for whether the system exhibits order or disorder.

3.4 Preliminary Data

Raw, preliminary data is presented in Figure 3.3. The intensity was measured in intervals of five degrees and simple lines were used to connect the points. The behavior is indeed flat for the control case (GFP Control) and oscillatory for the healthy

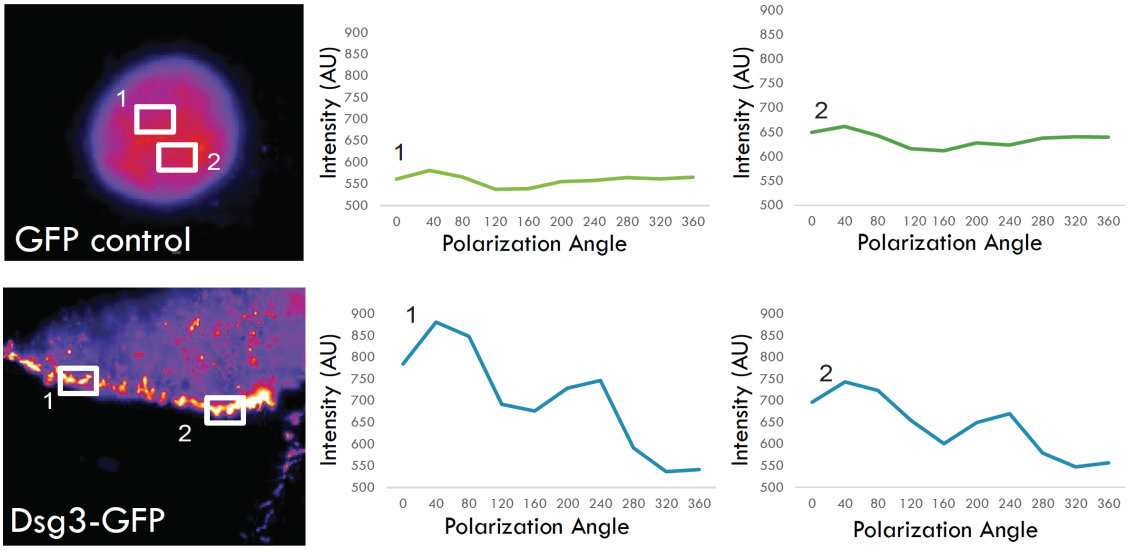

Figure 3.3: Intensity is plotted against excitation polarization angle for both a control case and healthy desmosome. We see that the control case data is more flat, while the desmosome data is oscillatory, albeit subject to minor declines from excessive measurement leading to photobleaching. Overall, however, this data is characteristic of the results we would expect based on our modeling.

desmosome; the steady decline, however, is due in part to photobleaching from excessive measurements, and reinforces our previous statement that we must use only a few measurements in our analysis. We expect that we would see behavior closer to our modeled results if we took only five measurements and applied our described method.

Chapter 4

Conclusion

The work presented here can be summarized by one fundamental idea: if there exists an inherent ordering in a biological system of interest whose components can be reliably tagged, then that ordering can be detected in that system with fluorescence polarization. This idea is powerful, for it gives us an avenue by which we can understand the organization of structures at the molecular level, and investigate dynamic changes in such systems.

We expect that researchers in this area will be able to move forward with gusto once they are able to fully resolve the actions of PV between binding and final disruption. Once the mechanisms are fully understood, we will be a step closer to developing targeted drugs and treatments for this currently untreatable disease that affects millions every year [4].

Once we show order is important with polarization, we will motivate future work to develop techniques to study order that do not involve tags or labels, thus allowing analysis in patients. Through the eyes of a clinician, this research can be used as a quick and non-invasive diagnostic tool to help assess whether a patient is infected with PV; by taking a few skin samples from the patient, tagging the membrane proteins of those samples, and imaging them, a preliminary guess can be made as to whether the sample exhibits order or disorder (e.g. whether the skin is healthy or diseased) and allow the practitioner to make a more informed decision on how to proceed.

The technique of fluorescence polarization microscopy is certainly not new, but the technique as applied to our system is indeed novel, as are our resulting analysis methods. These analysis methods were designed for this specific system, but could easily be extended to study other systems in which the specific ordering is thought to be critical to function, and where dynamic interaction is present. Depending on the system, the spatial derivation and intensity functions would need to be re-derived appropriately, but the method by which a cutoff is determined would be identical. Even the experimental method presented here would be acceptable for the system in question, provided that a sample from the system in question could be studied in vitro. Much like we have sought to understand the mechanisms of PV by considering the differences in ordering between healthy and diseased cells and allowing for dynamic observation, others could study the mechanisms of other diseases in different systems by considering the differences in ordering between the respective systems, once again with dogma of form defining function. Thus we would expect this technique would find a home in immunology and pathology.

Furthermore, because the structure of so many biological systems hinges on their intrinsic ordering, we expect that this optical technique and analysis will find its way into many fields of structural biology as a supplement for direct mechanical testing. It should serve as an effective verification of mechanical results and allow researchers in that area to put forward better evidenced conclusions.

We hope that this test can be used to develop further insights about the mechanisms of PV, and lead to diagnostic tools to aid patients. The next steps of course, are to complete our stated goal of filling a knowledge gap in this system by observing system dynamics and noting the behavior of the individual proteins. We will need to devise a method by which we can tie certain response patterns to real orientations within the cell so that we can make concrete statements about the spatial dynamics

therein.

For the future, we aim to find some means by which we can go beyond categorizing a desmosome as ordered or disordered and actually determine the given orientation. We also intend to improve our image analysis program in such a way that it can detect desmosome domains without manual guidance. We would also like to further sophisticate our model by allowing for internal individual variance; this would entail a system that exhibits general overall order, but allows slight spatial variation in its individual proteins.

Bibliography

[1] A. Al-Amoudi, D. Diez, M. Betts, and A. Frangakis. The molecular architecture of cadherins in native epidermal desmosomes. *Nature*, 450:832–7, 2008.

[2] A. Al-Amoudi and A. Frangakis. Structural studies on desmosomes. *Biochem Soc Trans*, 36:181–7, 2008.

[3] M. Amagai, V. Klaus-Kovtun, and J. Stanley. Autoantibodies against a novel epithelial cadherin in pemphigus vulgaris, a disease of cell adhesion. *Cell*, 67(5):869–77, 1991.

[4] A. Baroni, A. Lanza, N. Cirillo, G. Brunetti, E. Ruocco, and V. Ruocco. Vesicular and bullous disorders: pemphigus. *Dermal Clin.*, 25(4):597–603, 2007.

[5] A. Brodell and K. Rosenthal. Skin structure and function: The body's primary defense against infection. *Infectious Diseases in Clinical Practice*, 16(2):113–117, 2008.

[6] B. DeMay, N. Noda, A. Gladfelter, and R. Oldenbourg. Rapid and quantitative imaging of excitation polarized fluorescence reveals ordered septin dynamics in live yeast. *Biophys J.*, 101(4):985–94, 2011.

[7] D. Garrod and M. Chidgey. Desmosome structure, composition and function. *Biochim Biophy Acta.*, 1778(3):572–87, 2008.

[8] I Gladwell, J. Nagy, and W. Ferguson. *Introduction to Scientific Computing Using MATLAB*. Lulu Publishing, Internet, 2011.

[9] J. Jones, K. Yokoo, and R. Goldman. Further analysis of pemphigus autoantibodies and their use in stuides on the heterogeneity, structure, and function of desmosomes. *J Cell Biol.*, 102(3):1109–17, 1986.

[10] M. Jong. Shot noise emerges as metal wires go to shorter lengths. *Physics World*, 9(8):22–4, 1996.

[11] M. Kampmann, C. Atkinson, A. Mattheyses, and S. Simon. Mapping the orientation of nuclear pore proteins in living cells with polarized fluorescence microscopy. *Nat Struct Mol Biol. 2011*, 18(6):643–649, 2011.

[12] P. Koch, M. Mahoney, H. Ishikawa, L. Pulkkinen, J. Uitto, L. Shultz, G. Murphy, D. Whitaker-Menezes, and J. Stanley. Targeted disruption of the pemphigus vulgaris antigen (desmoglein 3) gene in mice causes loss of keratinocyte cell adhesion with a phenotype similar to pemphigus vulgaris. *J Cell Biol.*, 137(5):1091–102, 1997.

[13] A. Kowalczyk and K. Green. Structure, function, and regulation of desmosomes. *Prog Mol Biol Transl Sci.*, 116:95–118, 2013.

[14] A. Kress, P. Ferrand, H. Rigneault, T. Trombik, H. He, D. Marguet, and S. Brasselet. Probing orientational behavior of mhc class i proteins and lipid probes in cell membranes by fluorescence polarization-resolved imaging. *Biophys J.*, 101(2):468–76, 2011.

[15] A. Kress, X. Wang, H. Ranchon, J. Savatier, H. Rigneault, P. Ferrand, and S. Brasselet. Mapping the local organization of cell membranes using excitation-

polarization-resolved confocal fluorescence microscopy. *Biophys J.*, 105(1):127–36, 2013.

[16] W. Lea and A. Simeonov. Fluorescence polarization assays in small molecule screening. *Expert Opin Drug Discov. 2011*, 6(1):17–32, 2011.

[17] A. Mattheyses, M. Kampmann, C. Atkinson, and S. Simon. Fluorescence anisotropy reveals order and disorder of protein domains in the nuclear pore complex. *Biophys J.*, 99(6):1706–17, 2010.

[18] M. Maynadier, M. Chambon, I. Basile, M. Gleizes, P. Nirde, M. Gary-Bobo, and M. Garcia. Estrogens promote cell-cell adhesion of normal and malignant mammary cells through increased desmosome formation. *Mol Cell Endocrinol.*, 364:126–33, 2012.

[19] O. Nekrasova and K. Green. Desmosome assembly and dynamics. *Trends Cell Biol.*, 23(11):537–46, 2013.

[20] A. Shimizu, A. Ishiko, T. Ota, K. Tsunoda, M. Amagai, and T. Nishikawa. Igg binds to desmoglein 3 in desmosomes and causes a desmosome split without keratin retraction in a pemphigus mouse model. *J Invest Dermatol.*, 122(5):1145–53, 2004.

[21] L. Song, E. Hennink, I. Young, and H. Tanke. Photobleaching kinetics of fluorescein in quantitative fluorescence microscopy. *Biophys J*, 68(6):2588–2600, 1995.